

FORMATION FLYING FOR ALONG-TRACK INTERFEROMETRIC OCEANOGRAPHY – FIRST IN-FLIGHT DEMONSTRATION WITH TANDEM-X

Ralph Kahle⁽¹⁾, Hartmut Runge⁽²⁾, Jean-Sebastien Ardaens⁽¹⁾, Steffen Suchandt⁽²⁾, and
Roland Romeiser⁽³⁾

⁽¹⁾*DLR, German Space Operations Center (GSOC), 82234 Wessling, Germany,
Ralph.Kahle@dlr.de, Jean-Sebastien.Ardaens@dlr.de*

⁽²⁾*DLR, Remote Sensing Technology Institute, 82234 Wessling, Germany,
Hartmut.Runge@dlr.de, Steffen.Suchandt@dlr.de*

⁽³⁾*University of Miami, RSMAS-AMP, 4600 Rickenbacker Causeway, Miami, FL 33149, USA,
rromeiser@rsmas.miami.edu*

Abstract: *Beyond its primary mission objective, the TanDEM-X formation flying mission provides a unique test bed for demonstrating new SAR techniques such as Along-Track Interferometry (ATI) for ocean current measurement. In this paper we discuss the ATI formation control requirements and the limitations imposed by the implemented Helix-formation. We propose two ATI scenarios and verify their feasibility by means of software simulation and in-flight demonstration. In particular, flight results of the very first ATI experiment are presented, demonstrating the high potential of TanDEM-X for mapping ocean currents.*

Keywords: *formation flying, along-track interferometry, ocean current measurement*

1. Introduction

The TerraSAR-X mission (TSX, launched on 15 June 2007, operated in 505 km, sun-synchronous, low Earth orbit) provides high-resolution Synthetic Aperture Radar (SAR) data to both science and commercial users. At 21 June 2010 an almost identical satellite, TanDEM-X (TDX), was launched in order to form the first configurable SAR interferometer employing formation flying with TSX. The main objective of the common TanDEM-X (TerraSAR-X add-on for Digital Elevation Measurement) mission is to generate a global digital elevation model (DEM) with unprecedented accuracy as the basis for a wide range of scientific research as well as for commercial applications. In order to collect sufficient measurements for a global DEM, three years of formation flying are foreseen with changing across-track baselines ranging from 150 m to few kilometers [1].

Beyond that primary mission objective, the satellite formation provides a configurable SAR interferometry test bed for demonstrating new SAR techniques and applications. In particular, it offers a unique chance to measure very slowly moving sea ice as well as ocean currents by means of Along-Track Interferometry (ATI). Due to the importance of the DEM acquisition the first three years of the mission are executed with a formation optimized for this purpose. After finalization of the global DEM formation flying will be dedicated to a variety of scientific interferometric campaigns including ATI. However, during the first years of operation already thousands of data sets have been acquired in the course of the TanDEM-X Science Program [2].

Because of the fact that space-borne SAR ATI with along-track separations in the order of 50 m has not been demonstrated before, there is a strong interest in preliminary ATI experiments with TanDEM-X to validate the methods foreseen for both SAR acquisition and processing. In this

paper we demonstrate the possibilities and limits of along-track interferometry for ocean current measurements with the TanDEM-X mission from a flight dynamics perspective.

In chapter 2 we recall the formation flying concept (i.e. the relative eccentricity / inclination vector separation method) and the guidance, navigation and control approach implemented for TanDEM-X. In chapter 3 the formation control requirements for along-track oceanographic interferometry are derived. In contrast to the coarse 200 m along-track accuracy required for routine across-track interferometric global DEM acquisition, the along-track separation desired for ATI oceanography is only $50 \text{ m} \pm 10 \text{ m}$. This is quite challenging for ground control with typically 30 m RMS along-track control accuracy and maximum 100 m control error.

In chapter 4 we propose two options to realize along-track oceanographic interferometry with TanDEM-X, i.e. (1) the utilization of existing favorable formation geometries, and (2) an ATI campaign with along-track adjustments. The option (1) has already been demonstrated in March 2012 and flight results of the first ATI experiments for ocean surface current measurement at the Orkney Islands are presented. These measurements demonstrate the high potential of TanDEM-X for mapping water surface currents with high spatial resolution, which has applications in the field of optimal placement of renewable energy sites and to validate global circulation models which are used for climate research.

Finally, we present simulation results for option (2) employing the experimental TanDEM-X Autonomous Formation Flying (TAFF) system. TAFF makes use of nearly permanent onboard availability of real-time GPS-based relative navigation and autonomously plans and executes in-plane formation keeping maneuvers. It has successfully been validated in March 2011 and June 2012. The simulation results clearly demonstrate the precise formation control and reconfiguration capability. With TAFF future TanDEM-X ATI campaigns will become more flexible at the time when global DEM acquisition is finalized and formation geometries can be adjusted to the needs of oceanography and other secondary mission objectives.

2. The TanDEM-X Formation Flight

The acquisition of the TanDEM-X DEM requires the coordinated operation of two satellites flying in close formation. Several formation flying options have been investigated during the conceptual development phase, and the so-called Helix satellite formation has finally been selected for TanDEM-X [3]. The chosen formation geometry implies maximum out-of-plane (cross-track) orbit separation at the equator crossings and maximum radial separation at the poles. This is realized by small ascending node differences and by slightly different eccentricity vectors, respectively, as depicted in Fig. 1. This concept of relative eccentricity / inclination vector separation results in a Helix-like relative motion of the satellites along the orbit and provides a maximum level of passive safety in case of a vanishing along-track separation [4].

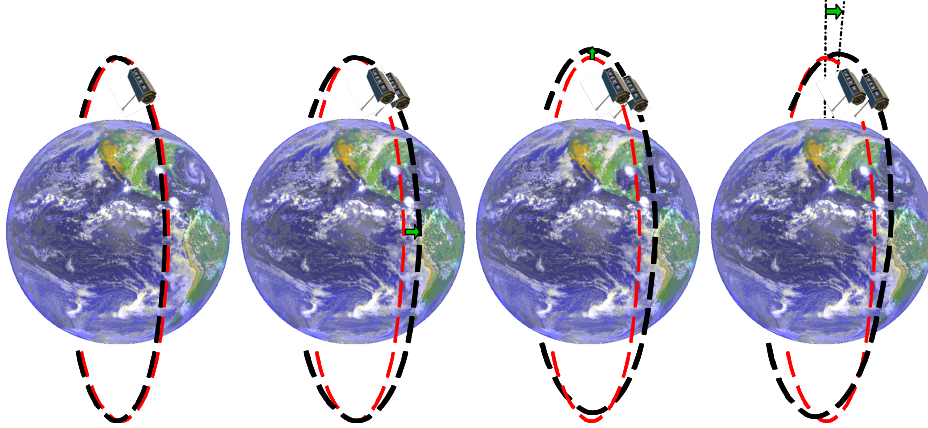


Figure 1. Formation building with relative eccentricity / inclination vector separation. From left to right: (1) identical orbits, (2) maximum horizontal separation at equator crossings by a small offset in the ascending node (green arrow), (3) a small eccentricity offset causes different heights of perigee / apogee and hence yields a maximum radial separation at the poles. (4) Optional rotation of the argument of perigee to achieve larger baselines at high latitude regions.

2.1. Guidance, Navigation and Control Concept

Within this paper the absolute orbit of a spacecraft is described in the Earth-centered-inertial reference frame by a set of six mean orbital elements, i.e. semi-major axis a (SMA), eccentricity e , argument of perigee ω , inclination i , right ascension of the ascending node Ω (RAAN), and argument of latitude u which is the sum of the argument of perigee and the mean anomaly, i.e. $u = \omega + M$. For near-circular satellite orbits, the Keplerian elements e and ω are commonly replaced by the singularity-free eccentricity vector $\vec{e} = (e_x, e_y)^T = e \cdot (\cos \omega, \sin \omega)^T$.

The relative motion of a chaser satellite (i.e. TDX) with respect to a target satellite (TSX) can be parameterized through an appropriate set of relative orbital elements which are obtained by the non-linear combination of the absolute orbital elements [4]:

$$\begin{pmatrix} \Delta a \\ a\Delta e_x \\ a\Delta e_y \\ a\Delta i_x \\ a\Delta i_y \\ a\Delta u \end{pmatrix} = \begin{pmatrix} a_{TDX} - a_{TSX} \\ a_{TSX} (e_{TDX} \cos \omega_{TDX} - e_{TSX} \cos \omega_{TSX}) \\ a_{TSX} (e_{TDX} \sin \omega_{TDX} - e_{TSX} \sin \omega_{TSX}) \\ a_{TSX} (i_{TDX} - i_{TSX}) \\ a_{TSX} (\Omega_{TDX} - \Omega_{TSX}) \sin i_{TSX} \\ a_{TSX} (u_{TDX} - u_{TSX}) \end{pmatrix} \quad (1)$$

with the relative semi-major axis Δa , the relative eccentricity vector $a \cdot (\Delta e_x, \Delta e_y)^T$, the relative inclination vector $a \cdot (\Delta i_x, \Delta i_y)^T$, and the relative mean argument of latitude $a \cdot \Delta u$. The relative e/i-vectors can be represented in either Cartesian or polar notation:

$$a\Delta\vec{e} = a \cdot \begin{pmatrix} \Delta e_x \\ \Delta e_y \end{pmatrix} = a \cdot \delta\vec{e} \cdot \begin{pmatrix} \cos \varphi \\ \sin \varphi \end{pmatrix} \quad \text{and} \quad a\Delta\vec{i} = a \cdot \begin{pmatrix} \Delta i_x \\ \Delta i_y \end{pmatrix} = a \cdot \delta\vec{i} \cdot \begin{pmatrix} \cos \theta \\ \sin \theta \end{pmatrix}. \quad (2)$$

The relative eccentricity vector with a length of $a \cdot \Delta e$ characterizes the periodic relative motion within the orbital plane. With otherwise identical orbital elements a , Ω and i (i.e. $\Delta a = 0$ and $a\Delta i = 0$) a pure eccentricity vector separation results in a relative orbit of TDX with respect to TSX forming an ellipse of dimension $\pm 2a \cdot \Delta e$ in the along-track direction and $\pm a \cdot \Delta e$ in the radial direction. In equation (2) the phase φ of the relative eccentricity vector is termed the relative perigee since at the mean argument of latitude $u = \varphi$ the chaser is located right below the target. In analogy with the relative eccentricity vector, the relative inclination vector can be employed to describe the relative motion in the cross-track direction by a harmonic oscillation of amplitude $a \cdot \Delta i$. The phase θ of the relative inclination vector in equation (2), called the relative ascending node, corresponds to the argument of latitude at which the chaser crosses the orbital plane of the target in ascending direction.

To avoid a collision hazard in the presence of along-track position uncertainties, care must be taken to properly separate the two spacecraft in radial and normal directions. As shown in [5] for geostationary satellites, this can be achieved by a parallel (or anti-parallel) alignment of the relative eccentricity and inclination vectors. This inherently safe formation flying concept is called relative eccentricity / inclination vector separation.

For monitoring purpose the relative orbital elements in equation (1) can be expressed in the Hill orbital frame (ΔR , ΔT , ΔN), which originates in the TSX Radial-Tangential-Normal (R-T-N) coordinate system. The Hill frame coordinates are determined from a set of constant relative orbital elements at $u_0 = 0$ by [4]:

$$\begin{pmatrix} \Delta R \\ \Delta T \\ \Delta N \end{pmatrix} = \begin{bmatrix} \Delta a & 0 & -a\Delta e_x & -a\Delta e_y \\ (a\Delta u + a\Delta i_y \cot i_{TSX}) & -3/2 \cdot \Delta a & -2a\Delta e_y & 2a\Delta e_x \\ 0 & 0 & -a\Delta i_y & a\Delta i_x \end{bmatrix} \times \begin{pmatrix} 1 \\ u - u_0 \\ \cos u \\ \sin u \end{pmatrix} \quad (3)$$

with the mean argument of latitude u as independent variable. Assuming Δa to be nominally zero, from equation (3) the maximum radial separation ΔR_{max} is found to be equivalent to the magnitude of the relative eccentricity vector, whereas the maximum normal separation ΔN_{max} equals the magnitude of the relative inclination vector. These maxima are also referred to as vertical separation $a \cdot \Delta e$ and horizontal separation $a \cdot \Delta i$, respectively. Typically, the TDX / TSX formation employed for routine bi-static radar acquisition consists of zero mean along-track separation, 250 to 500 m vertical separation and 150 to 500 m horizontal separation.

Figure 2 depicts the TDX-TSX formation geometry of February / March 2012 in the Hill orbital frame. Within one orbital period TDX performs one relative orbit about TSX too. The maximum along-track separation of 550 m is achieved at 30° and 210° argument of latitude or about $\pm 30^\circ$ geographic latitude.

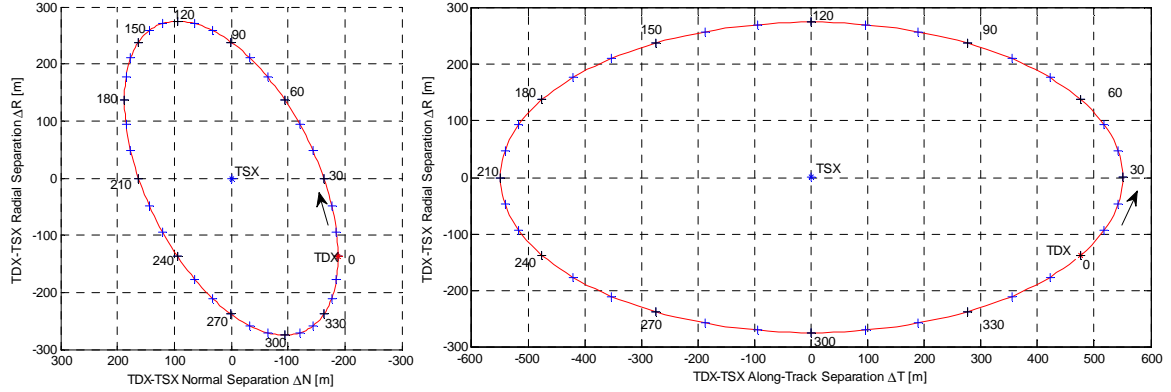


Figure 2. TDX-TSX relative motion in the Hill orbital frame: Radial-Normal separation (left) and Radial-Along-track separation (right). The formation geometry ($a \cdot \Delta e = 275\text{m}$, $a \cdot \Delta i = 188\text{m}$, $\varphi = 300\text{deg}$) was realized in the period from Jan. 12 to Mar. 29, 2012. The labels indicate the argument of latitude of the absolute orbit.

Due to the Earth oblateness, the relative eccentricity and inclination vectors are subject to secular perturbations. In particular, the relative eccentricity vector reflects the secular perigee variation of the individual satellites. It performs a rotation about the origin of the relative eccentricity vector plane with a period of roughly 100 days. This drift needs to be compensated by suitable formation keeping maneuvers to maintain a stable configuration. The maneuvers direction and size are determined in the Hill's orbital frame from the desired changes in the relative orbital elements by applying the simplified Gauss' equations [4]:

$$\begin{pmatrix} \delta \Delta a \\ a \delta \Delta e_x \\ a \delta \Delta e_y \\ a \delta \Delta i_x \\ a \delta \Delta i_y \\ a \delta \Delta u \end{pmatrix} = \frac{1}{n} \begin{bmatrix} 0 & 2 & 0 \\ \sin u & 2 \cos u & 0 \\ -\cos u & 2 \sin u & 0 \\ 0 & 0 & \cos u \\ 0 & 0 & \sin u \\ -2 & -3n(t-t_{\Delta v}) & -\sin u / \tan i \end{bmatrix} \begin{pmatrix} \Delta v_R \\ \Delta v_T \\ \Delta v_N \end{pmatrix} \quad (4)$$

with u being the mean argument of latitude of the maneuver, i.e. $u = u(t_{\Delta v})$, and n being the mean motion $n = (\mu/a^3)^{0.5}$ with $\mu = 398600.4415 \text{ km}^3/\text{s}^2$.

The required daily along-track velocity increment is proportional to the vertical separation $a \cdot \Delta e$. For example, a 300 m vertical separation demands every day two burns of approx. 0.5 cm/s each and separated by half a revolution. These maneuvers are additionally used to adjust the along-track separation and to compensate possible differential drag effects. In order to reduce the total maneuver size and improve the along-track control performance at the same time, the number of drift orbits in-between the maneuver pair has been introduced as a further variable in the on-ground maneuver planning process.

By means of Fig. 3 the in-plane control principle for formation maintenance can be further illustrated. The plot shows three pairs of cold-gas maneuvers (green verticals) and their impact on the formation. Every first maneuver occurs close to the violation of the lower limit of the relative argument of perigee φ (top) and resets φ close to its mean target value of 300 deg. As a result of this maneuver, the relative semi-major axis Δa will not remain close to zero (middle). The direction and magnitude of the first maneuver are chosen in order to adjust the relative

argument of latitude $a \cdot \Delta u$ and hence the mean along-track separation ΔT (bottom) within the short drift phase in-between the two maneuvers. In case of large $a \cdot \Delta u$ or ΔT offsets the nominal drift period of half an orbital period can be extended to 1.5 orbits or more to restore $a \cdot \Delta u$ in a faster way. The second maneuver completes the φ -adjustment to the upper control limit and brings Δa close to zero. A small Δa -offset is often used to yield an average zero ΔT error (bottom). The along-track error is the deviation of the real TDX-TSX along-track separation from the nominal one shown in the right of Fig. 2.

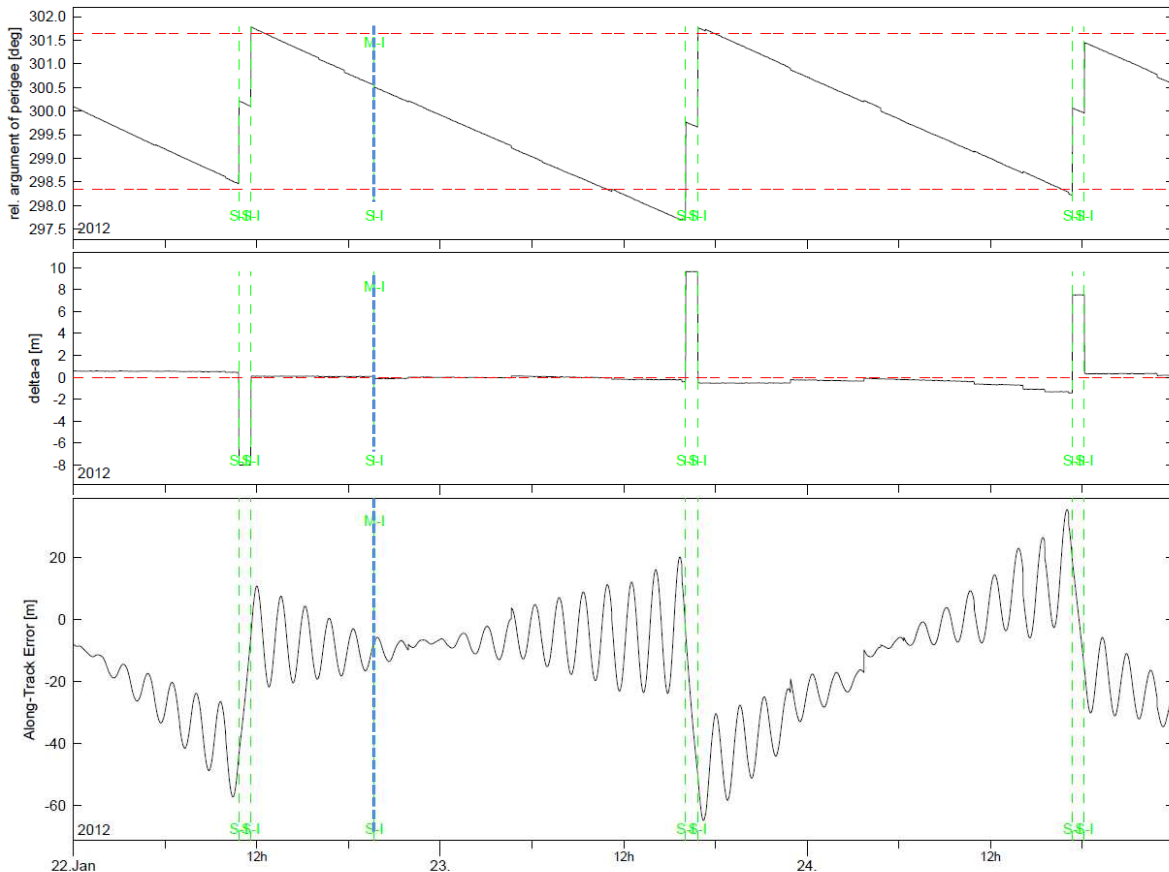


Figure 3. TDX-TSX in-plane relative motion observed during the period Jan. 22-25, 2012. From top to bottom: relative argument of perigee, relative semi-major axis, and relative along-track error. The dashed verticals indicate common TSX/TDX maneuvers (blue) and TDX formation keeping maneuvers (green).

2.2. Control Performance

Details on the routine ground formation control and first in-flight results have already been presented at the 22nd ISSFD in Brazil [6]. In the following only a brief summary on flight results relevant to ATI is given. A typical ground control performance is depicted in Fig. 4 and 5 for one 11-day cycle in Jan./Feb. 2012. Only the TDX-TSX along-track separation and error are depicted. The formation parameters during this cycle were $\varphi = 300$ deg, $a \cdot \Delta e = 275$ m, and $a \cdot \Delta i = 188$ m, which results in a ± 550 m nominal along-track separation (green line in Fig. 4).

Figures 5 and 3 (bottom) show the typical behavior of the along-track separation error. Referring to equ. (3) the observed drift after each maneuver pair results from the relative semi-major axis.

The short (orbit-) period oscillations are caused by the relative eccentricity vector deviation, which is zero in the middle of the maneuver cycle (i.e. for $\varphi = \varphi_{target}$).

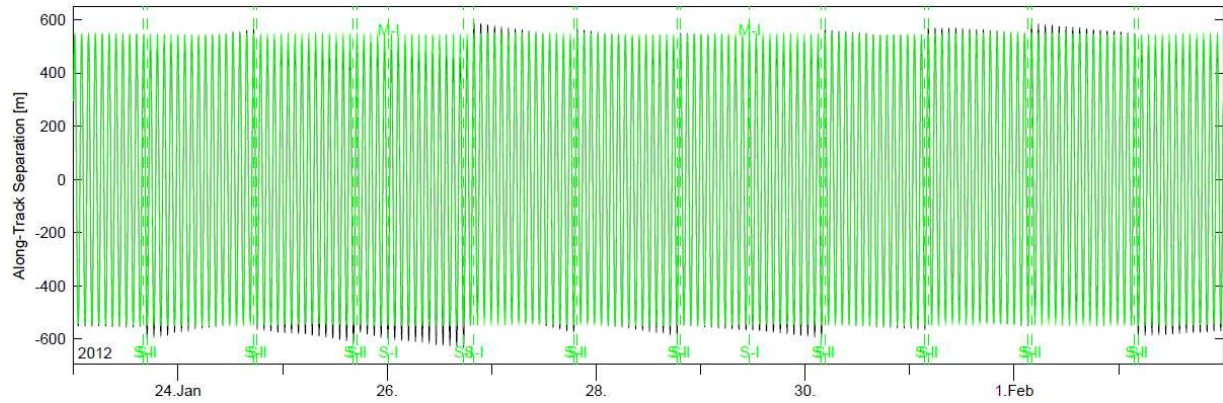


Figure 4. Nominal (green) and real (black) TDX-TSX Along-Track Separation in the period Jan. 23 – Feb. 3, 2012.

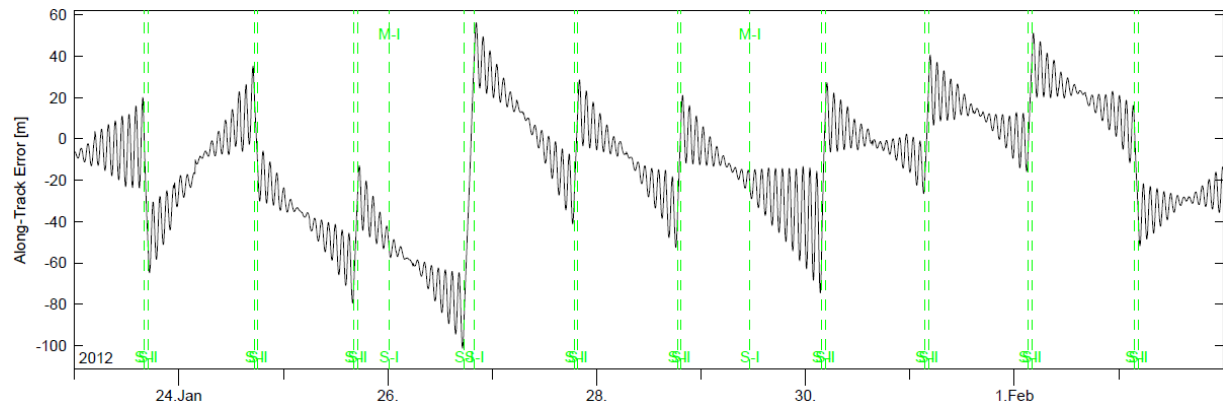


Figure 5. TDX-TSX Along-Track Error observed in the period Jan. 23 – Feb. 3, 2012.

From Fig. 5 we quantify the along-track control error over the 11-day interval as -12.9 m mean and 27.4 m standard deviation. Although the achieved control performance clearly satisfies the ± 200 m requirement for the DEM acquisition, it might not be sufficient for the purpose of ATI. The ATI constraints are derived in the following section.

3. Formation control requirements imposed by along-track oceanographic interferometry

TanDEM-X offers a unique chance to measure very slowly moving sea ice as well as ocean currents by means of Along-Track Interferometry (ATI). Oceanographic SAR interferometry is ideally acquired at an along-track separation of the two SAR sensors of about 40 to 60 m [7]. This range allows for ocean current velocity measurements with 0.1 m/s accuracy at an effective spatial resolution on the order of 100 m with a TerraSAR-X type SAR system. For smaller distances the signal-to-noise ratio decreases while for larger distances the reflected radar signal from the ocean surface might de-correlate (depending on the wind speed). In the following we consider along-track separations of 40 to 60 m as optimal separation for ATI and ranges of 10 to 40 m and 60 to 90 m as tolerable separations.

The satellites should fly exactly in the same track in order to avoid an across track separation which would form an additional across-track interferometer. The effects of ground topography

from the across-track interferometer and ground motion from the along-track interferometer would be superimposed in the radar instrument data and not easily separable. Fortunately the ocean doesn't show high topography but waves can distort the measurements if the across track separation is too large.

In [8] it was shown that a tight formation flight is feasible in general, if the satellites are equipped with sensors for relative navigation, bi-directional inter-satellite link and onboard autonomous formation control. The feasibility of close formation flights has successfully been demonstrated in several manned space flights, e. g. with the Space Shuttle and the International Space Station, and recently by the technology demonstration mission PRISMA [9]. However, the TSX and TDX satellites are not designed for such a close formation flight and they must be operated in the described inherently safe Helix formation with a 150 m minimum separation in the plane perpendicular to flight direction. As a drawback the Helix formation does not allow for a constant along track separation, in fact it varies by $\pm 2a \cdot \Delta e$. The challenge is to find an appropriate adjustment of the Helix formation parameters, that guarantees optimal along track separations for a wide range of geographical latitudes or to find means for a dynamical re-adjustment of the along track baseline.

In Tab. 1 we have summarized a selection of potential ocean energy sites in northern Europe and the Mediterranean Sea which could be observed with ATI. On every day of the 11-day repeat cycle of TerraSAR-X one particular site can be acquired. The two right columns will be explained in sect. 5 where a suitable formation flying scenario is simulated.

Table 1. Sample European ocean energy sites.

Site	Lat., deg	Long., deg	Acquisition epoch, Cycle day and UTC	ΔT_{nom} , m	ΔT_{offset} , m
Isles of Lewis, GB	57.72	-7.08	01 06:58:32	-14	-36
Orkney Islands	58.78	-3.11	02 06:41:03	-5	-45
Alderney, GB	49.72	-2.11	03 06:26:13	-90	+40
Channel	51.48	3.30	04 06:08:30	-76	+26
Kos, Greece	36.90	27.20	05 04:20:19	-213	+163
Faroer Islands	61.95	-6.81	06 07:06:01	29	+21
North Ireland	55.18	-6.23	07 06:50:36	-39	-11
Brest, France	48.37	-4.84	08 06:35:13	-105	+55
Herne Bay, GB	51.48	0.82	09 06:17:07	-76	+26
Kumkale, Turkey	40.00	26.25	10 04:28:04	-184	+134
Narvik, Norway	68.41	16.41	11 05:38:06	91	-41

The search for adequate formation geometries can be eased if the test sites on ground are grouped in regions of different latitudes. For this purpose we have grouped a number of potential ocean energy sites in Tab. 2. For simplicity we ignore the corresponding longitude, which of course has an impact on the mission planning aspects.

Table 2. Ocean energy site groups

Northern Europe	48 – 68 North	Madagascar	12 – 16 South
Mediterranean Sea	36 – 43 North	New Zealand	34 – 47 South

4. Options for ATI with TanDEM-X

Because of limited acquisition capacity the TanDEM-X secondary mission objectives cannot be realized before the completion of the global DEM acquisition, which is currently planned for end of 2013. Because of the fact that space-borne SAR ATI with along-track baselines in the order of 50 m has not been demonstrated before, there is a strong interest in preliminary ATI experiments with TanDEM-X to validate the methods foreseen for both SAR acquisition and processing. Within this chapter we investigate two options to realize oceanographic ATI with TanDEM-X. The first option can be considered as an experiment during the primary mission. The second option is intended as ATI campaign but allows for across-track interferometric observations too.

4.1. Option 1: Utilization of favorable formation geometry

To judge whether a particular formation used for DEM acquisition is suitable for ATI observations too we first have to determine the underlying along-track separation as a function of the geographic latitude. We consider the expression for ΔT in equation (3) and apply the following assumptions

- the target relative semi-major axis is $\Delta a = 0$, and
- the target mean along-track separation is $\Delta T = 0$ yielding $a\Delta u = -a\Delta i_y \cot i_{TSX}$

to yield the following relation:

$$\Delta T = -2 \cdot a \delta e \cdot \sin(\varphi - u). \quad (5)$$

The relation between argument of latitude u and geographic latitude ϕ is given as

$$\sin \phi = \sin u \cdot \sin i_{TSX} \quad (6)$$

with $i_{TSX} = 97.4$ deg. With these equations we can translate the formation geometries realized or planned in the period from 2010/12/12 to 2012/12/29 into the desired relation between along-track separation and geographic latitude as depicted in Fig. 6. The rectangles in Fig. 6 illustrate the oceanographic ATI sites from Tab. 2 with the optimal (green, i.e. $\pm(40..60\text{m})$) and tolerable (orange, i.e. $\pm(10..40 \text{ m})$ and $\pm(60..90\text{m})$) along-track separation, as described in sect. 3. It can clearly be seen that so far only two formation geometries have been realized which are suitable for oceanographic ATI. The first one (2011/11/18 – 2012/01/12) only grazes the relevant ATI region. However, the formation flown in the period from 2012/01/12 to 2012/03/29 clearly crosses one ocean energy site group of interest, i.e. northern Europe. This formation was both the tightest (i.e. 150 m minimum across-track separation) and the most tilted one. The geometry was primarily intended to acquire bi-static data-takes with very small across-track baselines implying a large height-of-ambiguity. This formation geometry is depicted in Fig. 2 too.

The tightest formation was chosen to demonstrate the possibilities and limits of the ATI method for ocean current measurements. A first set of ATI experiments was performed as Science data takes in February and March 2012 in the background of the on-going TerraSAR-X and TanDEM-X missions. At that time the ground-controlled formation geometry offered a favorable nominal TDX-TSX along-track separation of -5 m over one region of interest, i.e. the ocean current at the Pentland Firth between Scotland and the Orkney Islands at 59 deg northern latitude (cf. Tab. 1).

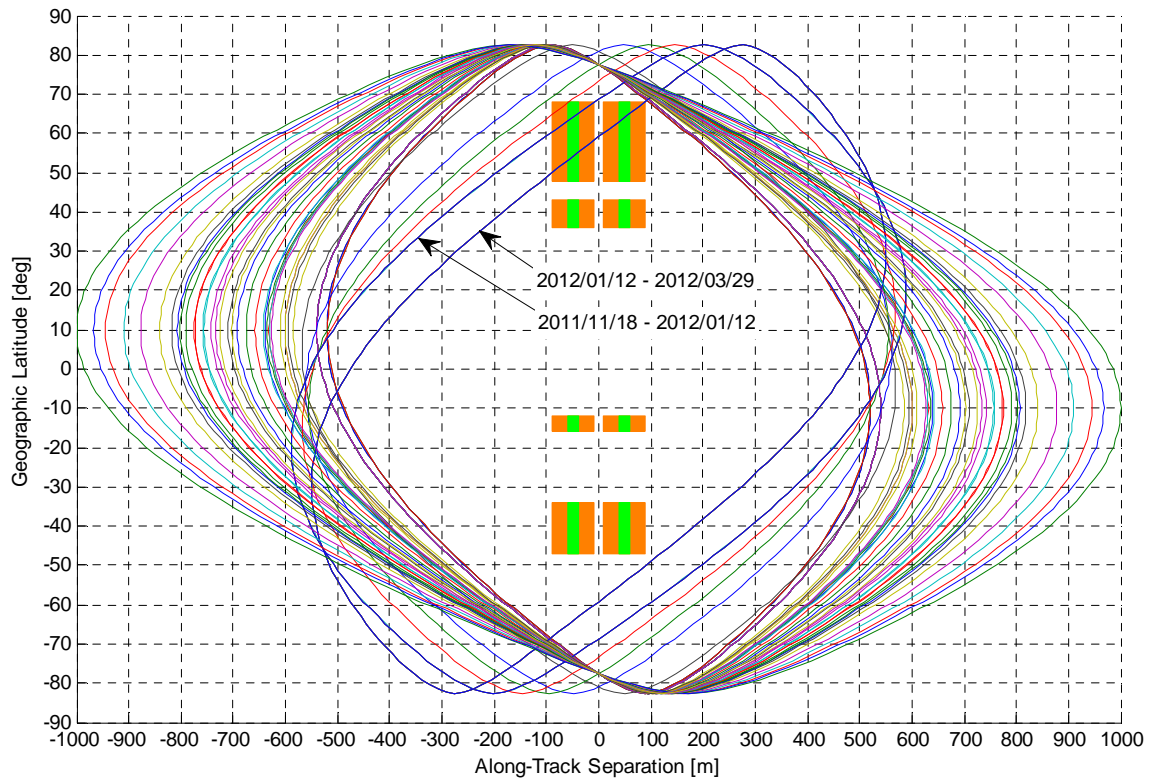


Figure 6. Geographic Latitude vs. nominal Along-Track Separation for all formation geometries in the period from 2010/12/12 to 2012/12/29. Each closed curve depicts one particular geometry valid for one or more 11-day cycles. Within one orbital revolution the closed curve is passed through in anti-clockwise direction. Descending orbits are in the left and ascending ones in the right. The rectangles illustrate oceanographic ATI site groups with optimal (green) and tolerable (orange) range in along-track separation.

Figure 7 depicts the achieved along-track separations in the descending orbit over 59 deg North within one 11-day cycle. It has to be noted that we have ignored the corresponding geographic longitude. Out of the 167 points shown in Fig. 7 only a few are relevant for observations at -3 deg West Longitude. The green and orange areas indicate optimal and tolerable ranges of TDX-TSX along-track separation. The routine ground-control achieved a -15 m mean separation with a standard deviation of 31 m. About one eighth of the potential flyovers met the optimal conditions.

To make sure that the TDX-TSX along-track separation was within the optimal range, the formation was manually controlled during this experiment. While the routine automated control process aims on a small mean along-track error over a 24 hour maneuver cycle, the manual process allows for small maneuver adjustments to achieve the desired along-track separation at a particular acquisition time without affecting the formation control accuracy.

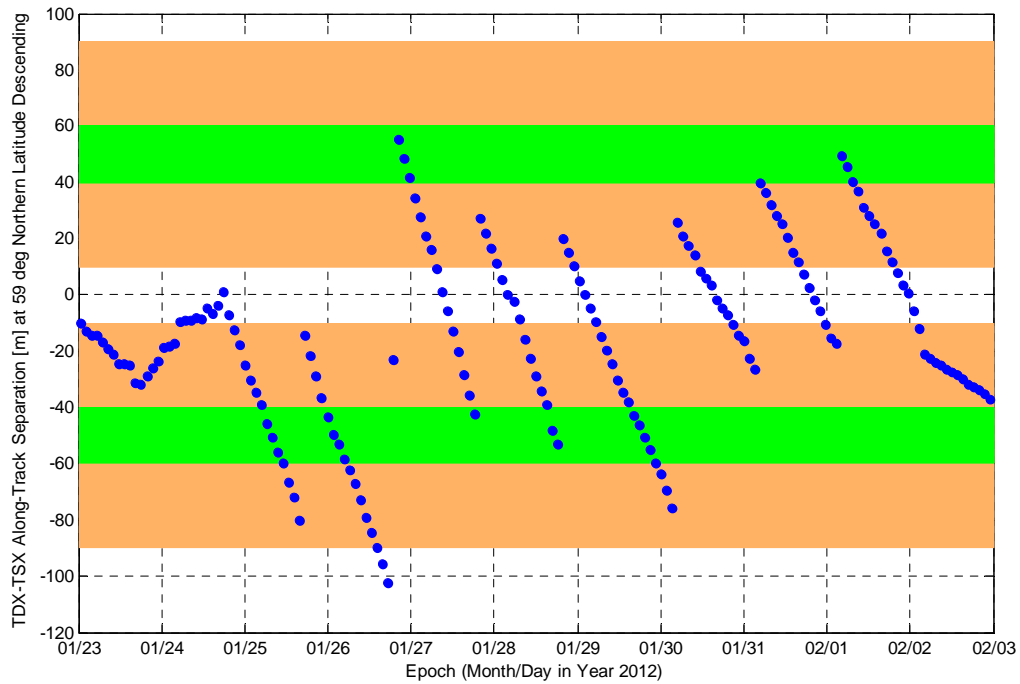


Figure 7. Achieved TDX-TSX along-track separations at 59.5 deg northern latitude in 167 descending orbits during the cycle from Jan. 23 to Feb. 3, 2012.

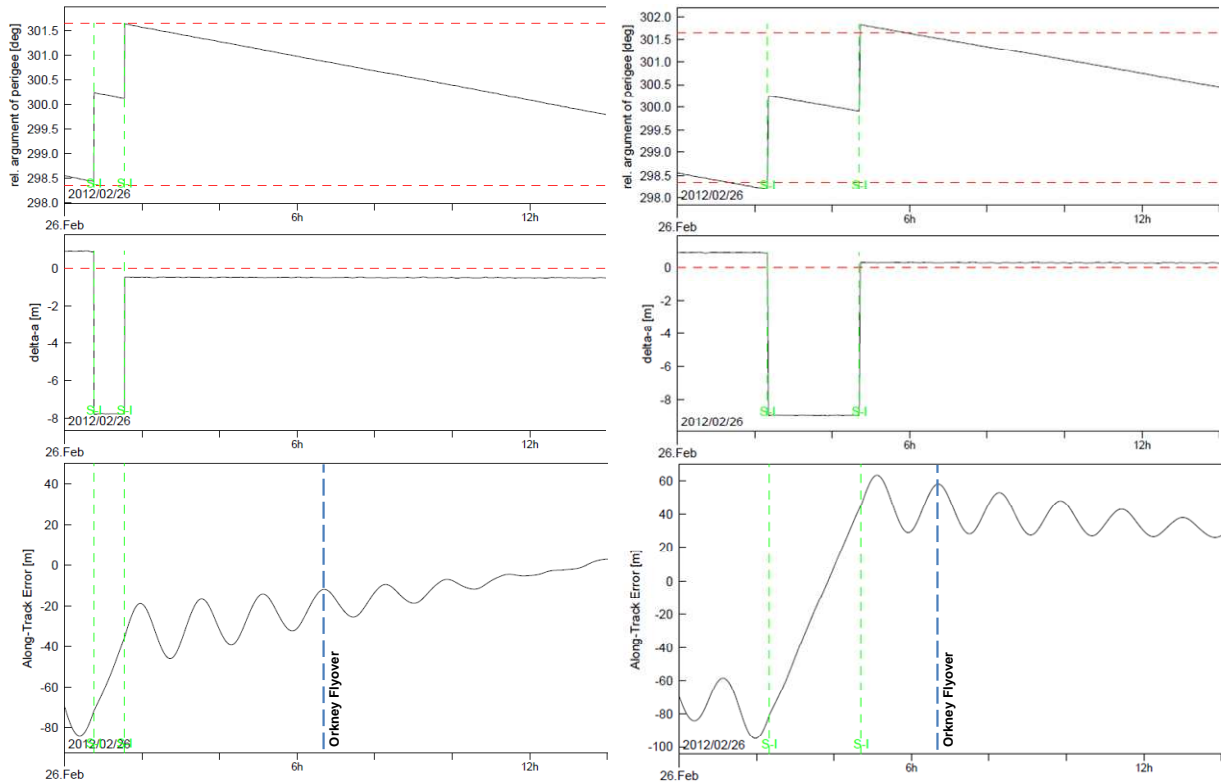


Figure 8. Nominal ground-autonomous (left) and realized manual (right) in-plane formation control for the Pentland Firth acquisition on Feb. 26, 2012.

In Fig. 8 we compare the in-plane control scenarios for the Pentland Firth acquisition on Feb. 26, 2012. The automated ground-control scenario is shown on the left side with cold-gas maneuvers at 0:45 and 1:32 UTC. The resulting along-track error is zero in the middle of a 24 hour maneuver cycle, i.e. 12 hours after the second maneuver (bottom). Contrary, the manual maneuver planning run depicted on the right side foresees cold-gas maneuvers at 2:19 and 4:41 UTC in order to install a slight along-track offset. Because of the fact that the total maneuver size is limited by the necessary correction of the relative eccentricity vector, a larger change of the along-track separation can only be realized by means of the drift time in-between the two maneuvers. The drift duration for the manual process was 1.5 orbits instead of 0.5 orbits.

It is important to point out that no additional fuel was spent, and more importantly, the formation flight foreseen for routine TerraSAR-X / TanDEM-X mission conduction was not disturbed, i.e. the 1-sigma formation control requirements were not violated by the experiment. At the moment of Orkney flyover an along-track separation of 52 m was installed by the manual process meeting the optimal range for ATI. For comparison, the default automated process would have installed a -19 m separation instead.

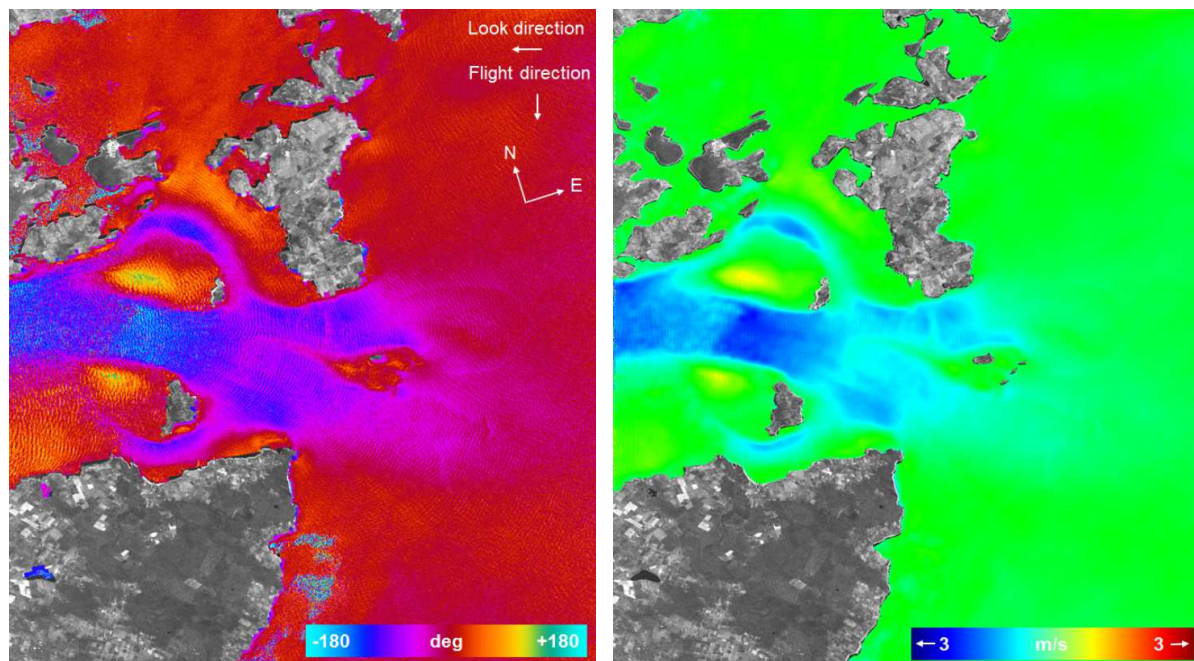


Figure 9. Color-coded interferometric phase (left) of a TanDEM-X acquisition of the tidal current between Scotland and the Orkney Islands [10]. The main surface movement is in westward direction. Land areas have been masked with the grey-scale SAR image. The phase can directly be converted into horizontal Doppler velocity (perpendicular to flight-direction) yielding a maximum velocity of 3 m/s (right).

Figure 9 depicts the first results of the ocean surface current mapping with TanDEM-X ATI [10]. The corresponding data take was acquired over the Orkney Islands on February 26th, 2012 at 6:41 UTC. The left image shows the interferometric phase after compensation of the average phase offset along the coast lines. Land areas have been masked with the SAR amplitude. The significant phase variations in the left and center parts of the image are caused by a tidal current directed away from the sensor as well as by wave motion. The TDX-TSX along-track separation was within the optimal acquisition range. The acquisition at 50 m separation yields a high

velocity-to-phase sensitivity and avoids de-correlation. The right image shows the ground-range Doppler velocity obtained from the ATI phase. The image clearly demonstrates the great potential of TanDEM-X for mapping water surface currents, which has applications in the field of renewable energy and climate research.

4.2. Option 2: ATI campaign with along-track displacement

Referring to Fig. 6 it becomes obvious that opportunities for oceanographic ATI acquisitions during the nominal TanDEM-X DEM acquisition phase are pretty rare. However, the number of ATI observations can significantly be increased by adjusting a single formation parameter: the mean along-track separation. For all scenarios depicted in Fig. 6 the target mean along-track separation is zero. For typical vertical separations between 200 and 500 m this yields a $\pm 400..1000$ m along-track motion with maximal separations close to the equator crossings. Here we have to consider that for separations larger than about 1 km the coherence might significantly degrade. So when adjusting the mean along-track separation to the ATI needs we have to ensure that the maximum along-track separation keeps below 1 km.

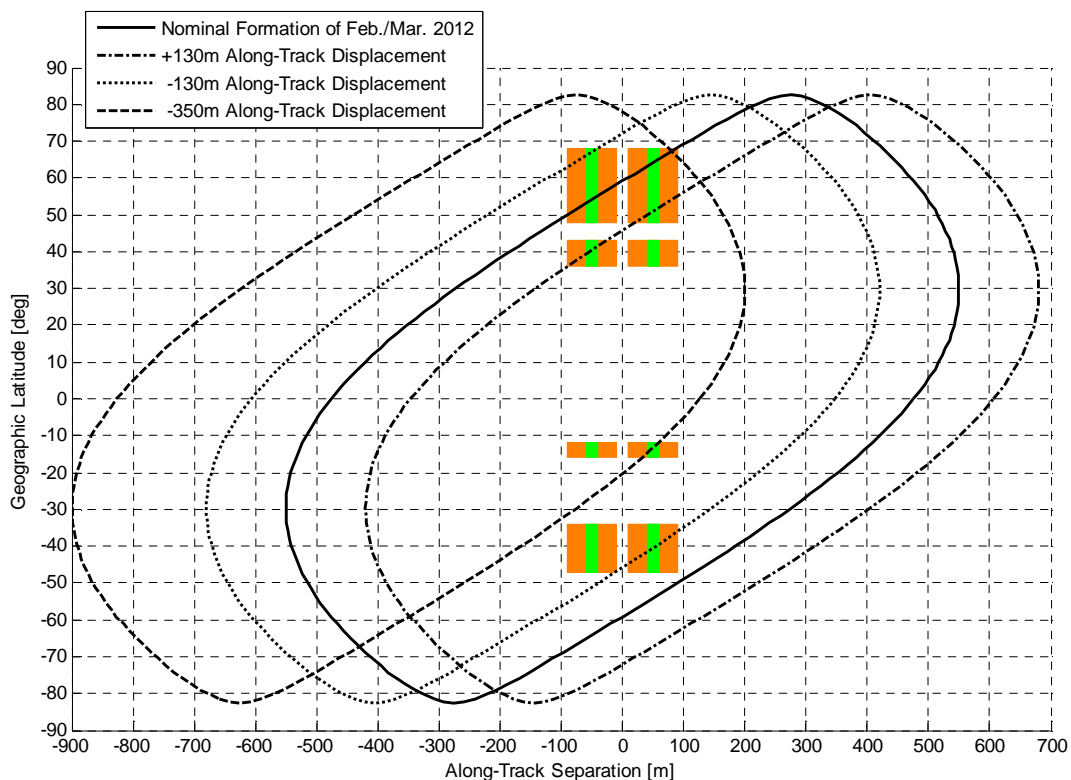


Figure 10. Possible adjustments of the formation geometry from Feb./Mar. 2012 (persistent line) by means of pure along-track displacement. The rectangles illustrate oceanographic ATI site groups with optimal (green) and tolerable (orange) range in along-track separation. The northern energy sites are acquired in descending orbits while the southern sites are observed in ascending orbits.

To illustrate the along-track displacement option we have chosen the same formation geometry as discussed in sect. 4.1, i.e. the geometry realized in Feb./Mar. 2012. In Fig. 10 we simulate the displacement of the nominal mean along-track separation by +130m, -130m and -350m. As a result, all energy site groups given in Tab. 2 could be observed with optimal ATI conditions. For

example, the -350m displacement would even allow for ATI observations at sites being close to the equator, e.g. Madagascar at 14 deg southern latitude. Of course, with a single formation geometry we can only achieve optimal ATI conditions at one or two particular latitudes (e.g. with +130m, dash-dot line in Fig. 10). Hence a real ATI campaign would comprise of several 11-day cycles with daily adjustments of the mean along-track separation. Such a scenario will be presented in sect. 5.

In order to proof the feasibility of this scenario a formation ground control simulation has been performed. The considered scenario deals with the epoch Feb. 26, 2012. The simulation results in Fig. 12 can directly be compared to the routine formation keeping scenario depicted in the left of Fig. 8 for the same day.

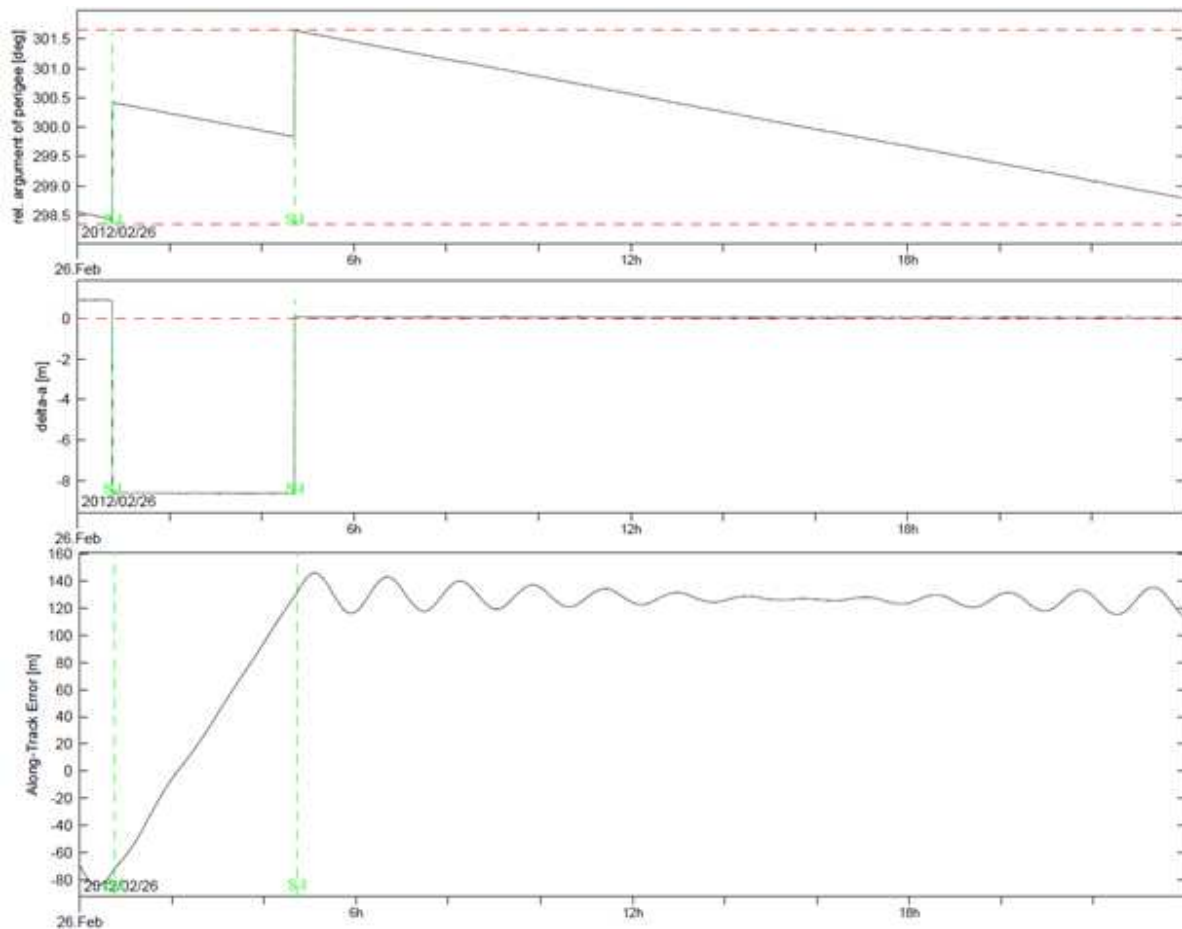


Figure 11. Simulated formation change to acquire a +130m mean along-track separation.

Since the campaign should not absorb additional fuel compared to the nominal formation flight, we have to benefit from an increased “drift” period in-between a formation keeping maneuver pair, which typically amounts to half orbital period. Within the simulation all formation target elements have been kept besides for the mean along-track separation, which is nominally zero and has been set to +130 m for the virtual ATI campaign. The “reconfiguration” is achieved by two maneuvers separated by 2.5 orbital revolutions. After execution of the 2nd maneuver (4:42 UTC) the targeted +130 m mean along-track separation is achieved and kept, see bottom of Fig. 11. Note that the relative argument of latitude (upper plot in Fig. 11) is controlled in the same

precise way as during routine formation maintenance (Fig. 8). No fuel in addition to the fuel needed for formation maintenance is required for this scenario. The cross-track formation geometry is not affected and routine cross-track interferometric acquisitions could be performed without limitation.

5. Future ATI campaigns with autonomous formation flying

The achievable formation control accuracy directly depends on the density of the used ground station network. This restriction can be overcome by means of onboard autonomous relative navigation and control. Employing the experimental TanDEM-X Autonomous Formation Flying (TAFF) system, the formation control cycle can be reduced from 24 hours to 5 hours. TAFF makes use of nearly permanent onboard availability of real-time GPS-based relative navigation and autonomously plans and executes in-plane formation keeping maneuvers. It has successfully been validated in March 2011 and June 2012 [11].

TAFF can be advantageously used for the purpose of along-track interferometry. Although TAFF doesn't implement any specific interface for dedicated ATI operations, a desired relative mean argument of latitude can be easily reached. In particular, a new nominal $a\Delta u$ can always be commanded from ground so that TAFF can slowly converge to the new formation configuration.

Based on the achieved TAFF in-orbit characterization a typical ATI scenario software simulation is conducted. The simulation set up comprises the same target formation parameters as used in the period February/March 2012, i.e. $\Delta a = 0$ m, $a\Delta e = 275$ m, $\varphi = 300^\circ$, $a\Delta i = 188$ m, $\theta = 90^\circ$, $\Delta T_{mean} = 0$ m (or $a\Delta u = 25$ m). The TAFF maneuver cycle is set to three orbits. The simulation covers an arbitrary 11-day period in April 2013. In order to observe the northern Europe targets given in Tab. 1 with optimal along-track separations (i.e. 40..60 m separation), the mean along-track separation offsets given in the right column of Tab. 1 are applied. The acquisition day 1 in Tab. 1 is equivalent to April 7, 2013 in the simulation. The new target parameters are "commanded" at 12:00 UTC.

Figure 12 depicts the simulation results. The green curve in the upper diagram shows the target mean along-track separations from Tab. 1. TAFF changes the along-track separation in a similar way as described for the ground control process. However, for TAFF the period in-between one maneuver pair is fixed to half orbital period. So the necessary along-track drift is installed by the first maneuver pair after commanding of the new target parameters, and stopped by the subsequent maneuver pair, i.e. after 3 orbits. In a worst case the new target parameters are activated shortly after the first maneuver, e.g. April 10 in Fig. 12. Then the new parameters are used by TAFF in the next planning cycle three orbits later. So without optimized planning it takes between 3 to 6 orbital revolutions to adjust the along-track separation.

The lower diagram in Fig. 12 depicts the achieved along-track control accuracy. Here the red lines indicate the acquisition epochs. Disregarding the periods of formation reconfiguration, a remarkable 5 m control accuracy can be achieved. Then, the along-track separation during ATI acquisitions would always be in the optimal range of 40 to 60 m. The simulation clearly demonstrates the great potential of TAFF for TanDEM-X ATI campaigns.

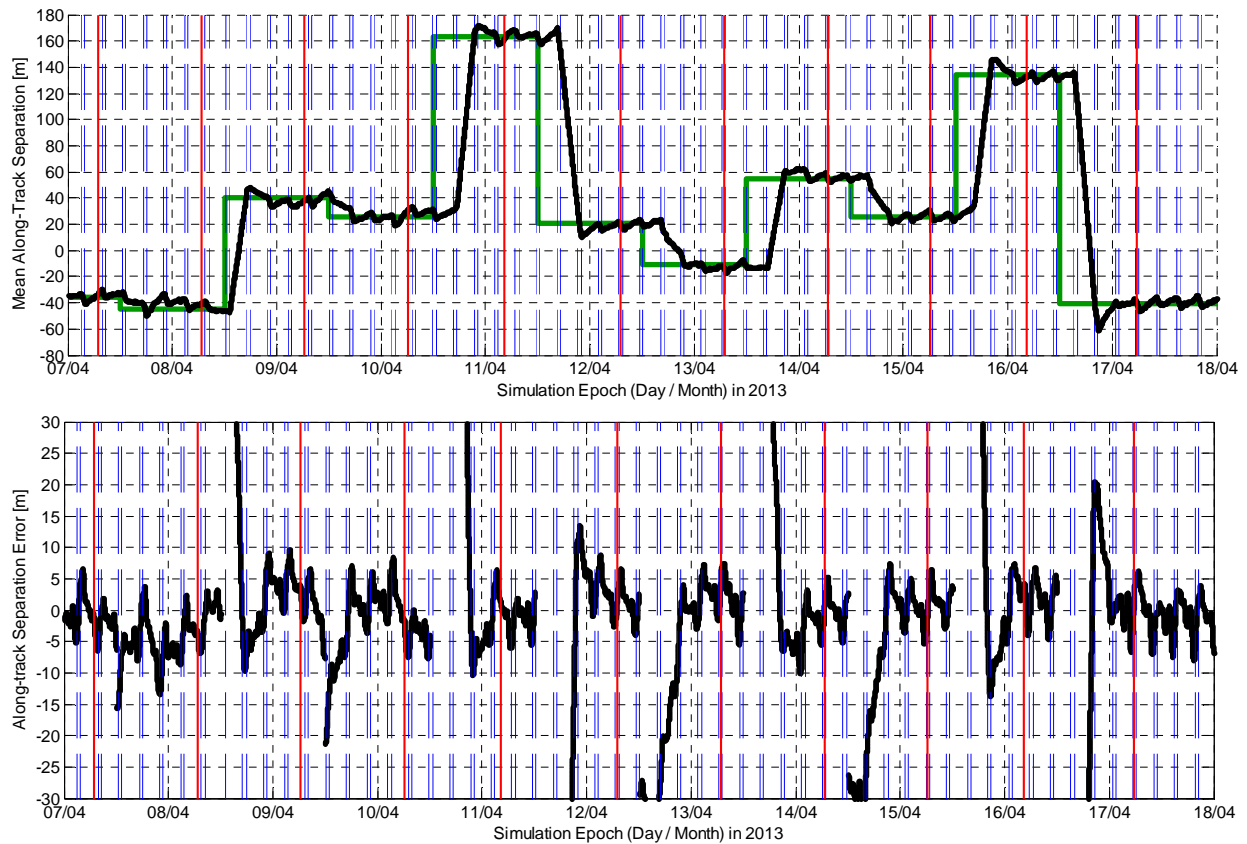


Figure 12. TAFF control performance in ATI mode: 11 day simulation with several reconfigurations of the relative mean along-track separation: Top: target (green) and simulated (black) mean along-track separation. Bottom: Achieved control accuracy. The TAFF maneuvers are depicted as dashed blue lines. The ATI acquisition epochs are marked as red lines.

6. Conclusions

The TanDEM-X formation flight is based on the concept of relative eccentricity / inclination vector separation. Despite the fact that the formation design is inherently safe and fully meets the needs of the primary mission objective, it certainly poses limitations to secondary mission objectives such as Along-Track Interferometry (ATI). In this paper we have discussed the limits and demonstrated the possibilities of ATI for ocean current measurements with TanDEM-X.

A first set of ATI experiments was performed in February and March 2012 in the background of the on-going TerraSAR-X and TanDEM-X missions. At that time the ground-controlled formation geometry comprised of minimum satellite distances of 150 m in the plane perpendicular to flight direction and favorable along-track separations over northern Europe. For the acquisition of the ocean current at the Pentland Firth on Feb. 26, 2012 the along-track separation was slightly adjusted to yield optimal observation conditions without affecting the routine DEM acquisition. The acquired data impressively illustrates the high potential of TanDEM-X for mapping water surface currents with high spatial resolution, which has applications in the field of optimal placement of renewable energy sites and to validate global circulation models which are used for climate research.

Furthermore we have conducted a software simulation to demonstrate future ATI campaigns with multiple targets by means of onboard autonomous relative navigation and control. The TanDEM-X Autonomous Formation Flying (TAFF) experiment is perfectly suited to conduct frequent along-track changes and precisely control the TDX-TSX along-track separation at the 5 m level.

7. Acknowledgement

The TanDEM-X project is partly funded by the German Federal Ministry for Economics and Technology (Förderkennzeichen 50 EE 0601) and is realized in a public-private partnership (PPP) between German Aerospace Center (DLR) and Astrium GmbH.

8. References

- [1] Krieger G., Moreira A., Fiedler H., Hajnsek I., Werner M., Younis M., Zink M., “TanDEM-X: A satellite formation for high-resolution SAR interferometry”, *IEEE Transaction on Geoscience and Remote Sensing*, Vol. 45, No. 11, pp. 3317–3341, 2010.
- [2] TanDEM-X Science Program web site: http://www.dlr.de/hr/en/desktopdefault.aspx/tabid-2317/3669_read-5492/
- [3] Fiedler H., Krieger G., and Zink M., “Constellation and formation flying concepts for radar remote sensing”, *Proceedings of advanced RF sensors for Earth observation, ESA/ESTEC, The Netherlands, 2006.*
- [4] D’Amico S., Montenbruck O., “Proximity operations of formation flying spacecraft using an eccentricity/inclination vector separation”, *Journal of Guidance, Control, and Dynamics*, Vol. 29, pp. 554–563, 2006.
- [5] Eckstein M.C., Rajasingh C.K., Blumer P., “Colocation Strategy and Collision Avoidance for the Geostationary Satellites at 19 Degrees West”, *Proceedings of the 5th International Symposium on Space Flight Dynamics, Toulouse, France, 1989.*
- [6] Kahle R., Schlepp B., Kirschner M., “TerraSAR-X/TanDEM-X Formation Control - First Results from Commissioning and Routine Operations”, *Proceedings of the 22nd International Symposium on Spaceflight Dynamics, Sao Jose dos Campos, Brazil, 2011.*
- [7] Romeiser R., Runge H., “Theoretical Evaluation of Several Possible Along-Track InSAR Modes of TerraSAR-X for Ocean Current Measurements”, *IEEE Transaction on Geoscience and Remote Sensing*, Vol. 45, No. 1, pp. 21–35, 2007.
- [8] Gill E., Runge H., “Tight Formation Flying for an Along-track SAR Interferometer”, *New Opportunities for Space. Selected Proceedings of the 54th International Astronautical Federation Congress; Acta Astronautica*, Vol. 55, pp. 473-485, 2004.
- [9] D’Amico S., Ardaens J.-S., Larsson R., “Spaceborne Autonomous Formation-Flying Experiment on the PRISMA Mission”, *Journal of Guidance, Control, and Dynamics*, Vol.35, pp. 834-850, 2012.
- [10] Suchandt S., Runge H., “First Results of TanDEM-X Along-Track Interferometry”, *IEEE. International Geoscience and Remote Sensing Symposium, Munich, Germany, 2012.*
- [11] Ardaens J.S., D’Amico S., Fischer D., “Early Flight Results from the TanDEM-X Autonomous Formation Flying System”, *Proceedings of the 4th International Conference on Spacecraft Formation Flying Missions & Technologies, St-Hubert, Quebec, Canada, 2011.*